SPACE WEATHER HAZARDS AND RESPONSES OF THE COUPLED MAGNETOSPHERE-IONOSPHERE SYSTEM DURING THE MAY 2024 GEOMAGNETIC STORM

Amarjargal BAT-ERDENE, Munkhzul JARGALNEMEKH, Sukhbaatar USNEKH, Gantsogt SUKBAATAR

Institute Astronomy and Geophysics, Mongolian Academy of Science (amarjargal98@iag.ac.mn)

ABSTRACT

A major geomagnetic storm, globally designated as the "Mother's Day Storm," occurred on May 10–11, 2024, marking the most severe geomagnetic storm event observed worldwide since 2003. This study comprehensively investigates space weather hazards by utilizing in situ satellite measurements, a global network of geomagnetic observatories, the regional MAG-HVD magnetic station, and GNSS receiver database inputs to examine the dynamic perturbations within Earth's magnetosphere and ionosphere in detail.

The "Mother's Day Storm" was driven by successive coronal mass ejections (CMEs), which caused the solar wind speed to exceed 1000 km/s, proton density to increase above 60 cm^{-3}, and dynamic pressure to sharply escalate up to 60 nPa. Consequently, the interplanetary magnetic field (IMF) Bz component underwent severe fluctuations, plunging to -40 nT, which triggered a robust convection process within the ionosphere and drastically accelerated plasma flow velocities. A profound interaction manifested within Earth's magnetosphere, with the geomagnetic activity SYM-H index dropping to an extremely intense peak of -518 nT (Dst = -412 nT) and the planetary Kp index reaching an extreme value of 9. In the ground based observatories recorded data of magnetic components, electron density significantly depleted at geomagnetic latitudes exceeding 50° during the geomagnetic storms main phase.

This high latitude ionospheric particle deficit (negative ionospheric storm) manifested as a dramatic drop in Total Electron Content (TEC) to 10-25 TEC, which rapidly expanded equator ward to encompass the midlatitude zone. Conversely, during the geomagnetic storms recovery phase, an phenomenon was observed where the Total Electron Content (TEC) returned to 40-42.5 TEC. These empirical findings demonstrate that during such severe space weather hazards, the near Earth space environment drastically alters, establishing highly hazardous conditions capable of inducing regional communication blackouts, degrading satellite operations, and causing critical disruptions to the reliability of GNSS/GPS navigation systems.

Keywords: Space weather hazard, Geomagnetic storm, Convection, Interplanetary Magnetic Field (IMF), Total Electron Content (TEC), Ionosphere

INTRODUCTION

- **Dynamic Structure of the Magnetosphere:** The Earth's magnetic field is not a simple dipole structure; it is continuously modified by the solar wind, forming a highly dynamic
- **Radiation Belts and CMEs:** The radiation belts (Van Allen belts) within the magnetosphere shield the Earth from hazardous cosmic radiation. When a Coronal Mass Ejection (CME) reaches the Earth's magnetic field, it alters the movement of particles within these belts, triggering a geomagnetic storm.
- **Ionospheric Storms:** During a geomagnetic storm, the massive energy from the solar wind interacts with the ionosphere, leading to complex phenomena where plasma density either sharply increases (positive ionospheric storm) or decreases (negative ionospheric storm).
- **Aim of the Study:** To investigate the spatial and temporal dynamic variations of ionospheric plasma flow and Total Electron Content (TEC) during the "Mother's Day Storm" (May 10-11, 2024) the strongest geomagnetic storm since 2003 (Kp = 9, SYM/H = -518 nT using satellite and ground-based (GNSS, MAGDAS) station data, and to evaluate

DATA AND METHODOLOGY

To evaluate the hazard levels of the May 10-11, 2024 geomagnetic storm, the following parameters were compiled and processed:

- **Solar Wind and Interplanetary Magnetic Field (OMNI):** Data from the Wind satellites were analyzed to capture hazardous spikes in solar wind velocity, proton density, and dynamic pressure.
- **Geomagnetic Activity Indices:** Hazardous fluctuations in the geomagnetic field were evaluated using the SYM/H, Dst, and global geomagnetic storm threat indices (Kp = 9).
- **Ground-Based Magnetometer data (MAGDAS / Khovd Station):** High-resolution variations in the horizontal (H), vertical (Z), and declination (D) components of the geomagnetic field over Mongolia were monitored.

Ionospheric Perturbations (GNSS-TEC): Total Electron Content (TECU) data from the International GNSS Service (IGS) network were processed to assess direct causes of geomagnetic signal delays

RESULTS AND DISCUSSION

Solar wind data, (Omni)

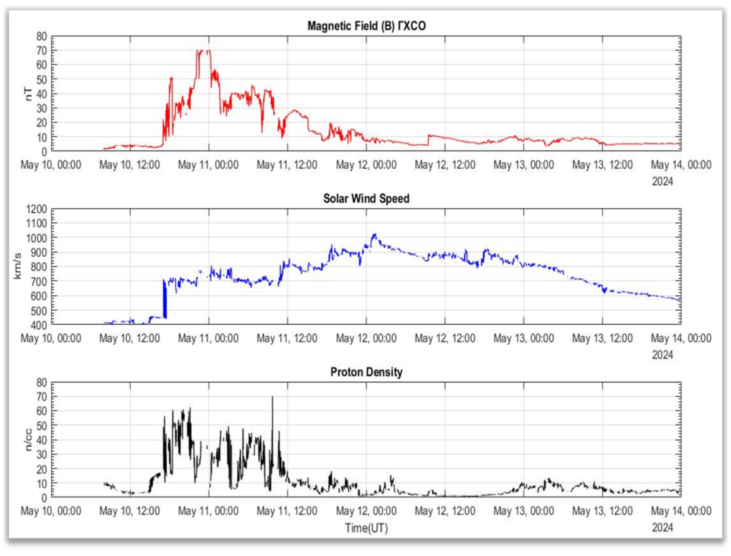

Figure 1

First we use the interplanetary magnetic field (IMF) in geocentric coordinates from the 1 min resolvution OMNI data set. The Omni IMF data are shifted from the observation points to the EART's bow shock nose. During the storm, solar wind speed surged past 1000 km/s, proton density exceeded 60 cm-3, and dynamic pressure soared above 60 nPa, signaling an immense influx of electromagnetic energy toward Earth. The southward Interplanetary Magnetic Field component (Bz) plunged to -40 nT, breaking through Earth's magnetic shielding. Consequently, the SYM/H index reached -518 nT and the Dst index hit -412 nT, entering critical threat levels.

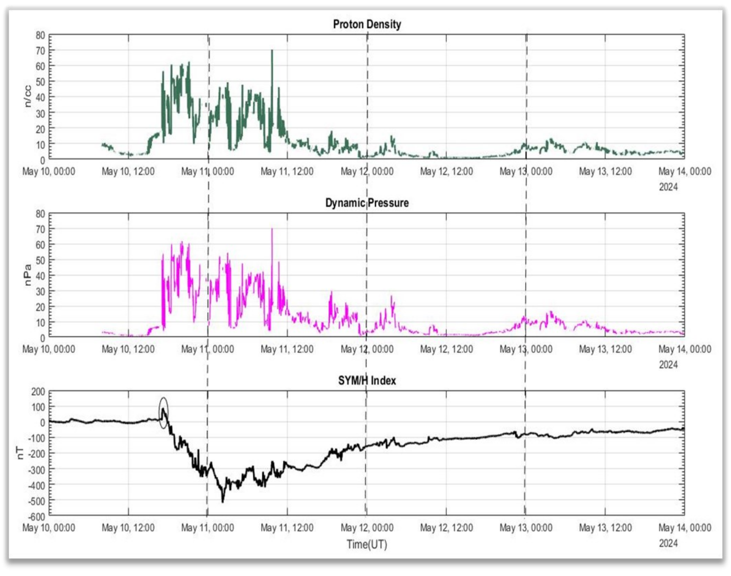

Figure 2

In figure 2 we show of geomagnetic storm on May 10–11, 2024, showing the storm sudden commencement (SSC), main phase, and recovery phase using Dst activity and SYM/H indices, along with dynamic pressure of solar wind and density variations from satellite data plotted against magnetic activity

Ground-Based Magnetometer data (MAGDAS - Khovd

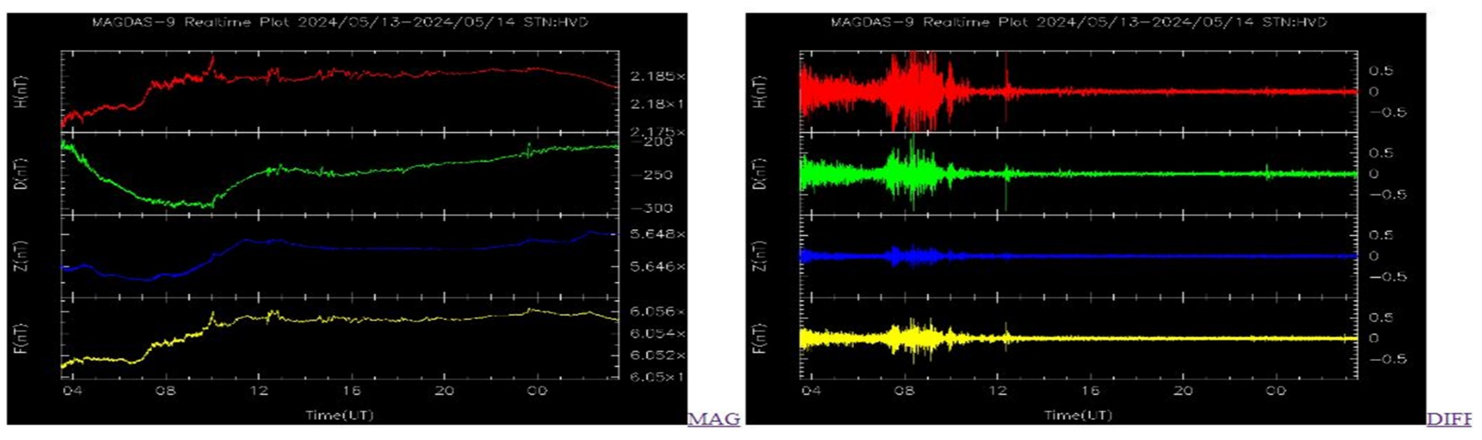

Figure 3

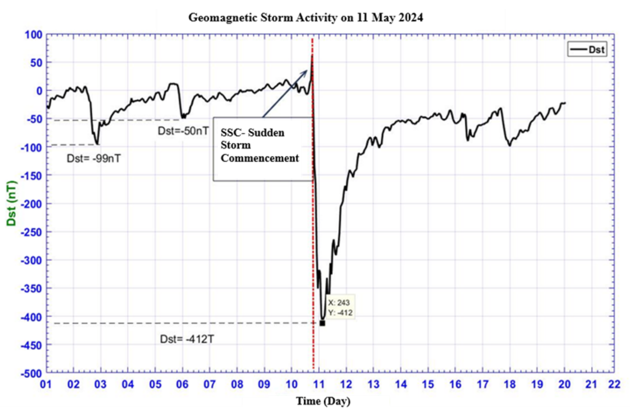

Figure 4

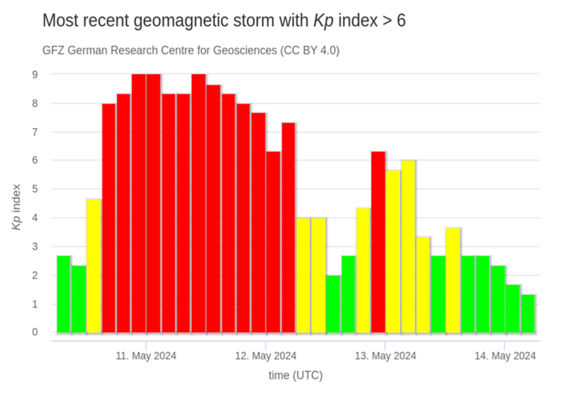

Figure 5

Observation from magnetometer at the Khovd station revealed a drastic drop of **-400 to -412 nT** in the horizontal component (H) magnetic field. This sharp negative excursion reflects the intense buildup of global ring currents and hazardous induced geoelectric currents

	Period (May 2024)	Parameter and Index	Observed Value	Hazard & Risk Level
1	May 10–11	*Kp* -index	9	Extreme Threat (Maximum geomagnetic storm rating)
2	May 11 (02:14 UT)	SYM/H D*st* -index	-518nT-412 nT	Severe ring current stress; risk of Geomagnetically Induced Currents (GICs)
3	May 10–11	Solar Wind-Speed (V*sw*)	> 1000 km/s	Mechanical and electrical surface-charging hazards for spacecraft
4	May 11–12	Ionospheric TEC	20–22.5 TECU	Plasma depletion (Negative storm)-High frequency radio scattering & blackouts
5	May 13–16	Ionospheric TEC	45–55.5 TECU	Plasma accumulation (Positive storm)-Severe GPS/GNSS signal propagation delay

Ionospheric disturbances and technological risks (GNSS-TEC)

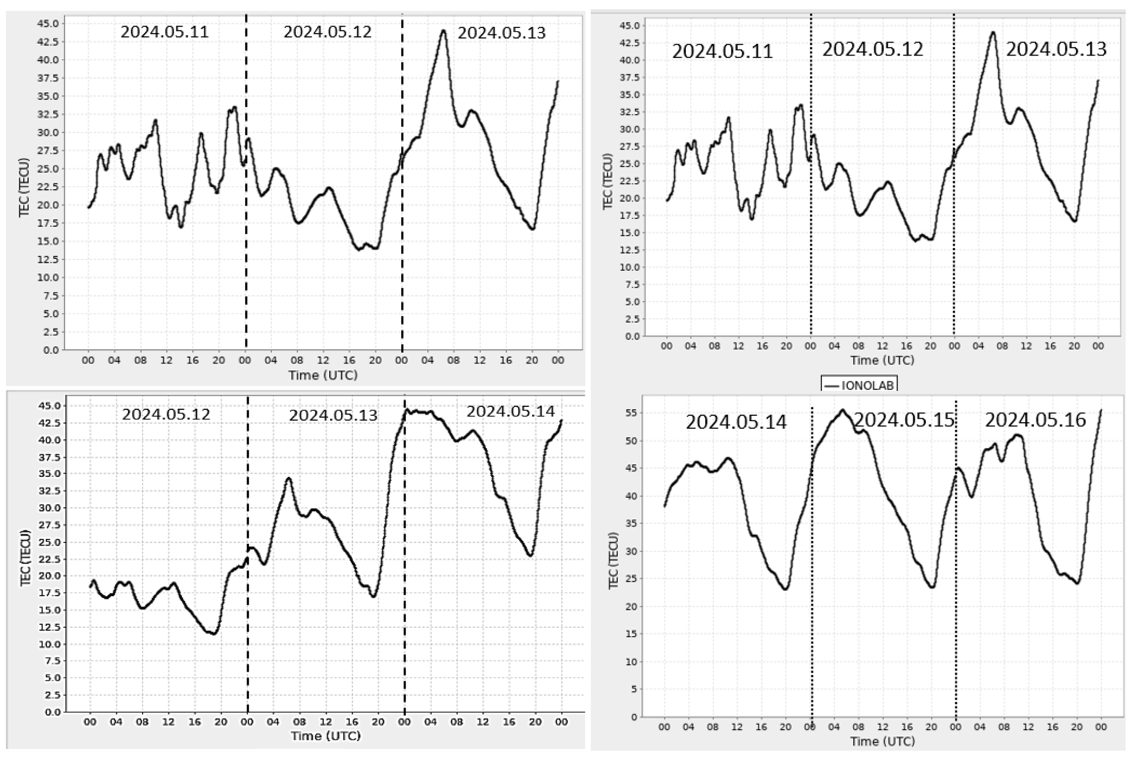

Figure 6

Geomagnetic forcing triggered a two-phase hazardous evolution in the ionosphere:

- **Plasma Depletion** / Negative Storm (May 11–12): At the peak of the storm, TEC dropped to 20–22.5 TECU. During this phase, the ionosphere's ability to reflect radio waves was severely degraded, causing HF radio communication blackouts.
- **Plasma Accumulation** / Positive Storm (May 13-16): As the storm transitioned into its recovery phase, TEC values surged to 45-55.5 TECU and remained elevated for 2-3 days. This heavy concentration of free electrons caused significant geomagnetic signal delays, introducing severe positioning errors in GPS navigation systems

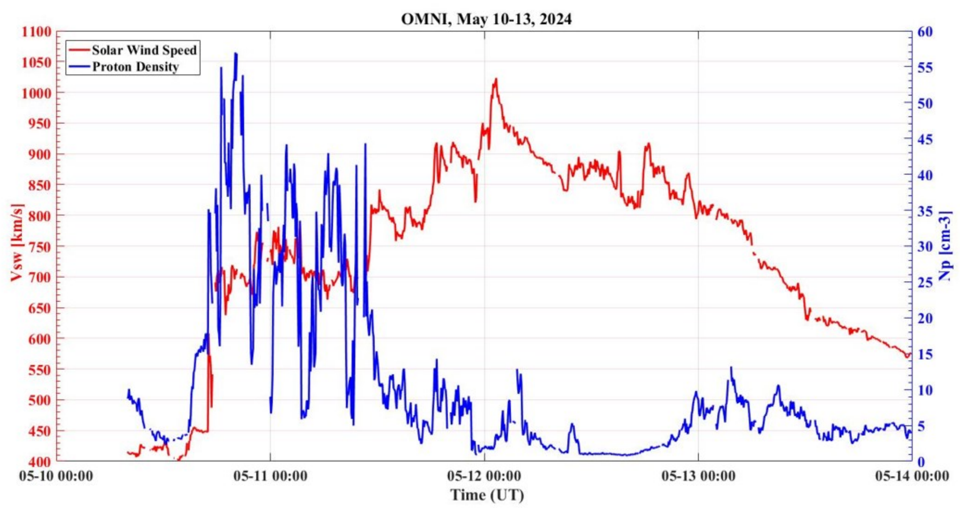

https://upload.wikimedia.org/wikipedia/commons/6/64/Solar_Storm_of_May_10%2C_2024_over_Viola%2C_Arkansas.jpg

When studying the changes observed on satellite observations during this geomagnetic storm, which reflect the dynamic variations of the ionosphere and magnetosphere as well as the physical phenomena occurring within these atmospheric layers, the plasma flow decreases significantly at dawn and dusk sectors. Ground-based observations show that at magnetic latitudes above 50°, the electron density noticeably decreases during strong geomagnetic storms. This density depletion originates from the early morning high-latitude region around the polar cusp. Under the strong influence of the solar wind, strong convection phenomena occur, which are thought to affect the plasma speed and atmospheric composition in the ionosphere. The region of reduced plasma density is not restricted to the polar cusp, but expands into the auroral zone and mid-latitude regions. The depleted plasma density persists for about 3 days before returning to pre-storm levels.

SUMMARY

The investigation of the May 2024 "Mother's Day Storm" underscores that severe geomagnetic storms pose direct, immediate hazards to modern critical infrastructure:

- Technological Risks: Within hours of storm onset, ionospheric structures were disrupted, creating conditions that directly compromised GPS/GNSS positioning accuracy and degraded aviation and maritime radio communications.
- Monitoring and Safety: Continuous multi-instrument monitoring of space weather and rapid geomagnetic variations is essential to provide early warnings and mitigate operational risks for satellite operators, power grids, and navigation-dependent systems.

ACKNOWLEDGEMENTS

I would like to thank Institute of Astronomy and Geophysics of MAS, Institute of Physics and Technology of MAS who cooperated in everything during the research work, Department of Physics of NUM and the Department of Geology and Geophysics of NUM. We acknowledge data from Omni https://cdaweb.sci.gsfc.nasa.gov,, World Data Center for Geomagnetism, Kyoto (WDC), data for INTERMAGNET and data Mongolian observatory Tavan Tolgoi(MTT). Thanks to ISSI-BJ space science to learn from and work with the worldwide famous scientists.

REFERENCES

Akasofu, S.-I. (1981). Energy coupling between the solar wind and the magnetosphere. *Space Science Reviews 1981 Vol. 28 Issue 2* , 121-190.
Amarjargal.B. (2019). Multi instrument observations of Patrick storm. *Takong ISSI-BJ MAGAZINE №12*, 12.
Baker, D. N. (2004). An extreme distortion of the Van Allan belt arising from the "Halloween" solar storm in 2003. *Nature, 432(7019)*, 878-881.
Buonsanto. (1999). Ionosheric storms. *Space science Reviews 88(3-4)*, 563-601.
Dungey.J.W. (1961). Interplanetary magnetic field and auroral zones. *Physical review letters*, 6-47.
Gonzalez, W. D. (1999). What is geomagnetic storm. *Journal of Geophysical Research: Space Physics*, 99(A4), 5771-5792.
King, J. P. (2005). Solar wind spatial scales in and comparisons of hourly Wind and ACE plasma and magnetic field data. *JGR, Space physics,* , 110(A2).
Parker, E. N. (1958). *Interaction of the solar wind with the geomagnetic field.* The Physics of Fluids, 1(3), 171-187.
Prölss, G. W. (2008). Physics of the Earth's space enviroment . *Springer*, introduction.
Ratovsky, K. G. (2018). Ionospheric responce to geomagnetic storms at mid-latiludes:Experimental result and modeling. *Advenced in Space Research, 61(7)*, 1816-1827.
Sojka, J. J. (1994). Ionospheric response to the March 1989 great magnetic storm: Modeling the F region. *Journal of Geophysical Research: Space Physics 99(A11)*, 21341-21352.
Tsyganenko, N. A. (2002). A model of the near magnetosphere with a dawn-dusk asymmetry . *Journal of Geophysical Research: Space Physics* , 107(A8).
Van Allen, J. A. (1959). Radiation around the Earth to a radial distance of 107,400 km. . *Nature, 183* , 430-434.
Wood, A. G. (2022). Global ionospheric variability and its drivers. *Journal of Atmospheric and Solar- Terrestrial Physics, 233*, 105829.